

# Optimization of enrichment and pretreatment of low-activity radium isotopes in the open ocean

Guiyuan Dai<sup>1, 3</sup>, Guizhi Wang<sup>1, 2, 3\*</sup>, Qing Li<sup>1, 3</sup>, Weizhen Jiang<sup>1, 3</sup>, Fei Zhang<sup>1, 3</sup>

<sup>1</sup> State Key Laboratory of Marine Environmental Science, Xiamen University, Xiamen 361102, China

<sup>2</sup> Fujian Provincial Key Laboratory for Coastal Ecology and Environmental Studies, Xiamen University, Xiamen 361102, China

<sup>3</sup> College of Ocean and Earth Sciences, Xiamen University, Xiamen 361102, China

Received 27 May 2022; accepted 13 September 2022

© Chinese Society for Oceanography and Springer-Verlag GmbH Germany, part of Springer Nature 2023

## Abstract

In the open ocean, radium isotopes are useful tracers of residence time and water-mass mixing. However, limited by the measurement resolution of commonly used gamma counters, the low activity of radium in the open ocean makes it necessary to enrich radium from large volumes of seawater and pretreat radium-enriched carriers prior to measurements. The commonly applied method of radium enrichment and pretreatment, however, has limitations of uneven coating of MnO<sub>2</sub> on cartridges, relatively expensive cartridges, time-consuming issues during cartridge-ashing, ash loss during transfer, and changes of gamma counters efficiency caused by different ash weights. To address these issues, in this study we optimized the enrichment and pretreatment of low-activity radium prior to measurements. Firstly, we replaced commonly used acrylic cartridges with cheaper polypropylene cartridges, which took 6 h to be ashed, 42 h shorter than for acrylic cartridges. Secondly, MnO<sub>2</sub>-coated cartridges were prepared with a circulating hot acidic KMnO<sub>4</sub> solution to ensure homogeneous coating. The radium extraction efficiency of this MnO<sub>2</sub>-coated cartridge was 20%–61% higher than that prepared by directly immersing cartridges in the solution. The radium delayed coincidence counter efficiency for MnO<sub>2</sub>-coated cartridge was stable with a moisture content of 0.05–1. Lastly, after ashing cartridges, instead of directly transferring the ash to a measurement vial, a mixture of hydroxylamine hydrochloride and hydrochloric acid was used to completely leach the ash for long-lived radium, followed by coprecipitation by BaSO<sub>4</sub>, to avoid potential loss of ash during transfer and variations in measurement geometry due to different ash weights. And the recovery of long-lived radium pretreatment was 94%–102%, which improved by 11% compared with the common method. In addition, the radium extraction efficiency of the MnO<sub>2</sub>-coated cartridge varied from 3% to 4% within the *in situ* pump working flow rate of 4–7 L/min, which fell within the measurement errors.

**Key words:** radium isotopes, MnO<sub>2</sub>-coated cartridge, enrichment of Ra, pretreatment of MnO<sub>2</sub>-coated cartridges, RaDeCC efficiency, extraction efficiency

**Citation:** Dai Guiyuan, Wang Guizhi, Li Qing, Jiang Weizhen, Zhang Fei. 2023. Optimization of enrichment and pretreatment of low-activity radium isotopes in the open ocean. *Acta Oceanologica Sinica*, doi: 10.1007/s13131-023-2152-3

## 1 Introduction

Radium (Ra) is a naturally occurring radioactive element with four isotopes, <sup>223</sup>Ra (half-life=11.4 d), <sup>224</sup>Ra (half-life=3.66 d), <sup>226</sup>Ra (half-life=1 600 a), and <sup>228</sup>Ra (half-life=5.75 a). Radium quartet has been widely employed in tracing submarine groundwater discharge and estimating residence time on nearshore, embayment, and shelf scales (Moore, 1996; Charette et al., 2003; Wang et al., 2014, 2015, 2018; Tan et al., 2018; Zhang et al., 2020). The long-lived radium isotopes, <sup>226</sup>Ra and <sup>228</sup>Ra, have been used to trace water masses and to estimate vertical and horizontal mixing rates in the open ocean (Moore, 1972; Trier et al., 1972; Sanial et al., 2018). However, <sup>228</sup>Ra activities in the open ocean are usually a few Becquerel per cubic metre (Ku et al., 1970; Charette et al., 2015; Kipp et al., 2018), in contrast to tens of Becquerel per cubic metre in coastal and shelf regions. Large volumes of seawater, several hundred liters, are, therefore, demanded to determine the activity of radium in the open ocean

waters due to the relatively low detection efficiency of commonly used gamma counters. Thus, limited by ship-time consuming collection of radium samples, short-lived radium isotopes in the open ocean, especially from deep below the surface, are rarely reported (Charette et al., 2015; Kipp et al., 2018).

In 1969, Moore presented a method of measuring <sup>228</sup>Ra in the seawater using a  $\beta$  counter via enrichment of radium by coprecipitation with BaSO<sub>4</sub>. His method required hundreds of liters of seawater for radium to be detectable and was too complicated to apply onboard (Trier et al., 1972; Kaufman et al., 1973). Then Moore and Reid (1973) found that MnO<sub>2</sub>-coated acrylic fibers performed well in scavenging radium from seawater at a relatively low flowing-through rate (<1 L/min). When sampling in the field, the MnO<sub>2</sub>-coated acrylic fibers had to be soaked in a predetermined position and it was difficult to determine the sampling volume (Moore, 1976). Moreover, such sampling was extremely time-consuming. Later on, *in situ* pumps

Foundation item: The National Natural Science Foundation of China under contract No. 41576074; the Natural Science Foundation of Fujian Province of China under contract No. 2019J01020.

\*Corresponding author, E-mail: [gzhwang@xmu.edu.cn](mailto:gzhwang@xmu.edu.cn)

were developed to extract radium at depth with Mn-impregnated acrylic cartridges at a relatively high flow rate, 5–10 L/min, (Michel et al., 1981). After enrichment of radium on the cartridge there are two ways of pretreatments in the laboratory. One is leaching the cartridge with hydrochloric acid (HCl) or nitric acid (HNO<sub>3</sub>) to recover the radium adsorbed on the cartridge (Moore, 1969). This pretreatment, however, was time-consuming with relatively low radium recovery. The other is ashing the cartridge and transferring the ash to a measurement vial (Henderson et al., 2013).

Therefore, MnO<sub>2</sub>-coated cartridges installed on *in situ* pumps have been widely used to extract radium from open-ocean seawaters and ashing has been a common pretreatment practice (Henderson et al., 2013; Charette et al., 2015; Sanial et al., 2018).

However, when we tested these procedures in our lab, some issues arose. Firstly, it was not easy to make MnO<sub>2</sub> evenly impregnated on the cartridge. Secondly, the long overnight baking time (about 48 h) was time-consuming. Thirdly, there was an ash loss when transferring the ash to a measurement vial. Lastly, the weight of the ash varied greatly from 1.7 g to 12.4 g, which would result in a change by 25% in the measurement efficiency of a gamma detector (Henderson et al., 2013). To address these issues, in this study, we aimed to optimize the methods of low-activity radium enrichment and pretreatment.

## 2 Materials and procedures

As shown in Fig. 1, our optimization of low-activity radium enrichment and pretreatment procedures include a change of the cartridge material, a design of a circulation coating system, and an additional treatment of the ashed cartridge. Briefly, we replaced acrylic cartridges with polypropylene cartridges and designed a KMnO<sub>4</sub> solution-circulating system to coat MnO<sub>2</sub> on the cartridge. In addition, the MnO<sub>2</sub>-coated cartridges were pretreated after ashing with leaching and coprecipitation of radium with BaSO<sub>4</sub> prior to measurements.

### 2.1 Preparation of MnO<sub>2</sub>-coated cartridges

We dissolved 474 g KMnO<sub>4</sub> (Xilong Scientific, China) in 5 L Reverse Osmosis (RO) pure water at room temperature and diluted 60 mL concentrated H<sub>2</sub>SO<sub>4</sub> (Guaranteed Reagent, Sino-

pharm Chemical Reagent, China) with 1 L pure water. Then the KMnO<sub>4</sub> solution was mixed with the diluted H<sub>2</sub>SO<sub>4</sub> solution in a beaker (5 L) to get a hot (70–80 °C) acidic (1%, *v/v*) KMnO<sub>4</sub> solution (0.5 L/min). The beaker with KMnO<sub>4</sub> solution was put in the water bath (HH-8, Bangxi, China) to keep the temperature at 70–80 °C. A blank cartridge (5 inches high, 5 mm in pore size, 60 mm in diameter, and made of polypropylene by Huamo Co., China) was put into a matching holder (Mianyang SINOMIX, China) and the hot acidic KMnO<sub>4</sub> solution circulated through the cartridge continuously with a submersible pump (JP-064, SUN-SUN, China) (Fig. S1). About an hour later, the cartridge was turned upside down to ensure an even coating of the cartridge with MnO<sub>2</sub>. Two and a half hours later, the circulation was stopped, and the holder was taken out. The cartridge was washed by connecting the inlet and outlet, respectively, of the holder to pure water until the water through the cartridge was colorless. The washing process took about 2 h. Then the cartridge was dried, which took about 2 d, and packed in a zip-lock bag. The entire process, including coating, washing and drying cartridges usually took more than 2 d.

### 2.2 Enrichment of radium and measurement of <sup>224</sup>Ra

To determine low-activity radium isotopes in the open ocean, *in situ* pumps (McLANE, America, Water Transfer System L V S/N: 11721) with MnO<sub>2</sub>-coated cartridges were used to enrich radium. The flow rate of the *in situ* pump ranged from 4 L/min to 7 L/min. After enrichment of radium, the MnO<sub>2</sub>-coated cartridge was washed with RO water at least three times as much as the volume of the cartridge holder to desalt thoroughly (Sun and Torgersen, 1998). And the moisture content (the mass ratio of the water to the MnO<sub>2</sub>-coated cartridge) of the MnO<sub>2</sub>-coated cartridge was adjusted to 0.05–1 with an air pump (ACO-003, SUN-SUN, China). Then <sup>224</sup>Ra absorbed by MnO<sub>2</sub>-coated cartridges was measured using a radium delayed coincidence counter (RaDeCC).

### 2.3 Pretreatment of MnO<sub>2</sub>-coated cartridges and measurement of <sup>226</sup>Ra and <sup>228</sup>Ra

After the measurement of <sup>224</sup>Ra, the MnO<sub>2</sub>-coated cartridges were measured for <sup>226</sup>Ra and <sup>228</sup>Ra with a high purity germanium

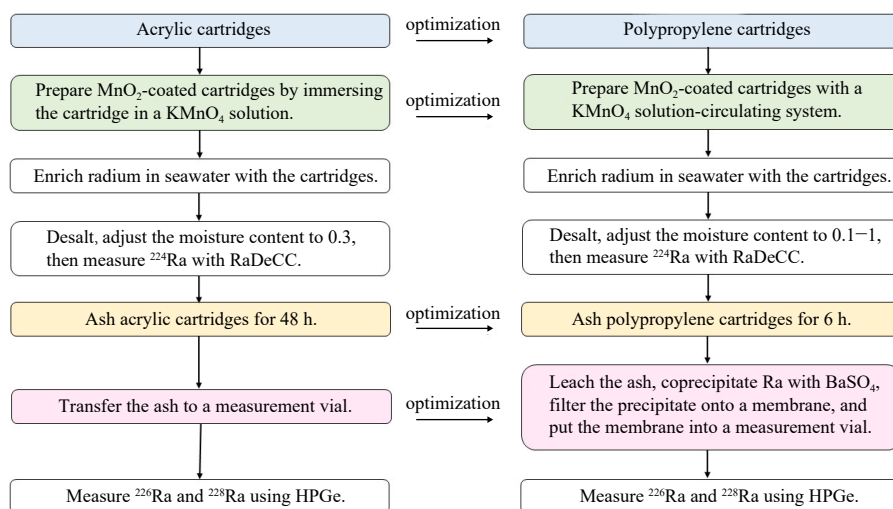
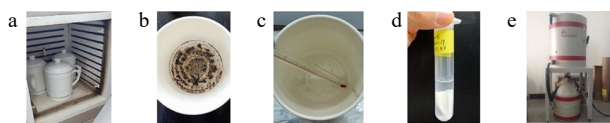


Fig. 1. Flowchart of low-activity radium enrichment, pretreatment, and measurement procedures in Henderson et al. (2013) (left) and in this study (right). RaDeCC denotes radium delayed coincidence counter. HPGe denotes high purity germanium gamma spectrometer.



**Fig. 2.** Pretreatment of  $\text{MnO}_2$ -coated cartridge and measurement of  $^{226}\text{Ra}$  and  $^{228}\text{Ra}$ . a. Ashing; b. the cartridge ash; c. leaching of the ashed cartridge; d. coprecipitate of  $\text{BaSO}_4$  with radium in a measurement vial; e. measurement of  $^{226}\text{Ra}$  and  $^{228}\text{Ra}$  using high purity germanium gamma spectrometer.

gamma spectrometer (HPGe) (GCW4023, Canberra, America). Firstly, the  $\text{MnO}_2$ -coated cartridge was ashed in a muffle furnace (KSL-1200X-M, Kejing, China) at  $820^\circ\text{C}$  for 6 h (Fig. 2a). The ash (Fig. 2b) was then leached with about 250 mL (more was used if necessary) heated ( $80\text{--}90^\circ\text{C}$ ) mixture of 1 mol/L hydroxylamine hydrochloride (Xilong, China) and 1 mol/L HCl (Guaranteed Reagent, Sinopharm Chemical Reagent, China) at a ratio of 2:1 until the ash was completely dissolved (Fig. 2c). After leaching, the mixture was diluted to about 600 mL with RO water, followed by coprecipitating radium in the solution with  $\text{BaSO}_4$  (with 25 mL 1 mol/L  $\text{NaHSO}_4$  (Xilong, China) and 5 mL saturated  $\text{Ba}(\text{NO}_3)_2$  (Xilong, China) added to the solution, which was then stirred with a glass rod until the precipitate was formed and the bottom was not seen). After standing for 12 h, the precipitate was filtered onto a  $0.45\ \mu\text{m}$  (smaller than the particle size of  $\text{BaSO}_4$ ) cellulose acetate membrane, which was folded and put in a 10 mL centrifugal vial and RO water was added to the scale of 4 mL (Fig. 2d). The vial was then sealed with parafilm for three weeks before being measured for  $^{226}\text{Ra}$  and  $^{228}\text{Ra}$  (Fig. 2e).

### 3 Assessments and discussion

#### 3.1 Improvements in the preparation of $\text{MnO}_2$ -coated cartridges

Henderson et al. (2013) suggested that an acrylic grooved cartridge (13 cm high) made by 3M Co. with a 48 h soaking period performed well in radium extraction. However, the acrylic grooved cartridge is relatively expensive. We replaced the acrylic cartridge with a cheaper polypropylene cartridge made in China (as described in Section 2.1).

To prepare  $\text{MnO}_2$  impregnated cartridges, we immersed the polypropylene cartridge in 0.5 mol/L acidic  $\text{KMnO}_4$  solution at  $70^\circ\text{C}$  to  $80^\circ\text{C}$  according to Henderson et al. (2013), and the soaking time was extended from 45 min based on Henderson et al. (2013) to more than 13 h. Unfortunately, only 0.7 g  $\text{MnO}_2$  was coated on the surface of this cartridge and internal adsorption of  $\text{MnO}_2$  was scarce (Fig. 3a). To address this uneven coverage issue, we developed a circulation system to allow  $\text{MnO}_2$  to adsorb on the cartridge homogeneously in 2.5 h (Fig. S1). Using this system, about 10 g  $\text{MnO}_2$  was adsorbed on the cartridge from inside out (Fig. 3b). The radium extraction efficiencies of the cartridge immersed in the  $\text{KMnO}_4$  solution for about 10 h (Fig. 3a) were

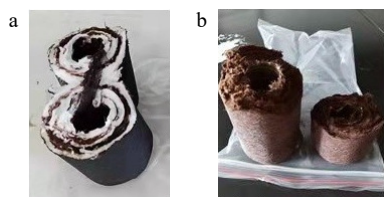


**Fig. 3.**  $\text{MnO}_2$ -coated cartridges made by immersing in a hot acidic  $\text{KMnO}_4$  solution (a), from the acidic  $\text{KMnO}_4$  solution-circulating system (b) shown in Fig. S1.

56%, 64% and 67% for  $^{224}\text{Ra}$ ,  $^{226}\text{Ra}$  and  $^{228}\text{Ra}$ , respectively, which were only equivalent to 62%–83% of that of the cartridge made using the circulation system (Fig. 3b).

#### 3.2 Determination of the RaDeCC efficiency for $\text{MnO}_2$ -coated cartridges

RaDeCC has been widely used as a convenient instrument to measure  $^{223}\text{Ra}$  and  $^{224}\text{Ra}$  (Rama et al., 1987; Moore and Arnold, 1996; Moore, 2008; Wang et al., 2015, 2018). After sampling, the initial  $^{224}\text{Ra}$ , including excess  $^{224}\text{Ra}$  and  $^{224}\text{Ra}$  supported by  $^{228}\text{Th}$ , was measured within 1–3 d. A month later,  $^{224}\text{Ra}$  supported by  $^{228}\text{Ra}$  was measured. The initial  $^{223}\text{Ra}$  (including excess  $^{223}\text{Ra}$  and  $^{223}\text{Ra}$  supported by  $^{227}\text{Ac}$ ) measurement was conducted within 7–10 d after sampling.  $^{223}\text{Ra}$  supported by  $^{227}\text{Ac}$  was measured in two months. Therefore, excess  $^{223}\text{Ra}$  and  $^{224}\text{Ra}$  were obtained through 4 measurements (Moore, 2008). The details of calculating the excess  $^{223}\text{Ra}$  and  $^{224}\text{Ra}$  can be found in Moore and Arnold (1996) and Moore (2008). In this study, the  $^{224}\text{Ra}$  standard for the  $\text{MnO}_2$ -coated fiber and  $\text{MnO}_2$ -coated cartridge was supported by its parent  $^{228}\text{Th}$ . Similar to the measurement of  $^{223}\text{Ra}$  and  $^{224}\text{Ra}$  on the  $\text{MnO}_2$ -coated fiber (Moore and Arnold, 1996), short-lived radium isotopes adsorbed by  $\text{MnO}_2$ -coated cartridges were also measured using RaDeCC. But the detector efficiency for  $\text{MnO}_2$ -coated cartridges was different from that for  $\text{MnO}_2$ -coated fibers due to shape difference, which caused difference in sweeping efficiencies of alpha particles. To determine the RaDeCC efficiency for  $\text{MnO}_2$ -coated cartridges, four cartridge standards for  $^{224}\text{Ra}$  were made. Because stock solution of  $^{227}\text{Ac}$  was not available, the standard for  $^{223}\text{Ra}$  was not discussed in this study. The activity of  $^{232}\text{U}$  stock solution (equilibrated with daughters  $^{228}\text{Th}$  and  $^{224}\text{Ra}$ ), which was used for  $^{224}\text{Ra}$  calibration, is  $(4.15 \pm 0.03)$  Bq/g. The  $^{232}\text{U}$  solution was diluted with about 2 L Ra-free seawater, and was then circulated through a  $\text{MnO}_2$ -coated cartridge driven by a peristaltic pump (07554-95, Cole-Parmer, America) for 1 h. The Ra-free seawater was made using surface seawater collected in the South China Sea in the summer of 2018, with a salinity of 33.2 and a temperature of  $19.5^\circ\text{C}$ , and  $\text{MnO}_2$ -coated fibers. Then the cartridge was washed well with 1 L RO water to remove the salt. The residual liquid from diluted  $^{232}\text{U}$  solution and washed RO water were merged and flowed through 16 g  $\text{MnO}_2$ -coated fibers at a flow rate less than 1 L/min to enrich radium (Moore, 1976). The  $\text{MnO}_2$ -coated fiber (with a mass ratio of water to fiber of 1) was immediately measured with RaDeCC to determine how much radium was not adsorbed on the  $\text{MnO}_2$ -coated cartridge. The radium on the  $\text{MnO}_2$ -coated fiber was below the detection limit, suggesting there was no radium in the residual liquid and washed RO water. Then the cartridge was stored in a zip-lock bag, waiting to be checked for temporal stability.

The relative standard deviation (RSD), which is the ratio of the standard deviation to the average, of the cartridge standard was used to test if the cartridge standard was stable based on the RSD of the fiber standard. In our laboratory, the  $\text{MnO}_2$ -coated fiber standard for  $^{224}\text{Ra}$  used for RaDeCC, which was from Willard S. Moore, University of South Carolina, has been used for more than 10 a and is stable. The fiber standard with moisture content of 1.0 was measured for a week to test the stability of RaDeCC (Fig. S2). Four RaDeCC systems were tested and the fiber standard was measured with each system for about 300 min once a day. In the first 100 min, the efficiency varied greatly until about 200 min. Thus, we suggest that the fiber standard should be measured for at least 200 min. Moreover, the efficiency varied among the four systems. The efficiency of System 2 was the lowest,  $0.441 \pm 0.003$ , while System 4 had the highest efficiency,  $0.520 \pm 0.005$ . For Systems 1 and 3, the efficiencies were  $0.499 \pm$

0.008 and  $0.509 \pm 0.008$ , respectively. The RSD of the fiber standard measured with the four systems was no more than 0.02 (Fig. S2). So, we assume the cartridge standard is practically stable if the RSD of the cartridge standard is less than 0.02.

Six months later, the four cartridge standards were measured with RaDeCC Systems 1, 2, 3, and 4 (Fig. 4). The RaDeCC efficiency varied slightly for the same RaDeCC system. The RaDeCC efficiency varied from 0.279 to 0.295, with an average of  $0.284 \pm 0.005$  for RaDeCC System 1, from 0.251 to 0.262, with an average of  $0.257 \pm 0.003$  for RaDeCC System 2, from 0.323 to 0.336, with an average of  $0.331 \pm 0.004$  for RaDeCC System 3, and from 0.304 to 0.320, with an average of  $0.310 \pm 0.005$  for RaDeCC System 4 (Fig. 4). All the RSDs were no more than 0.02. Thus, the cartridge standards were stable. The RaDeCC efficiency for cartridges of the four systems was 0.257–0.331, 35%–43% lower than that for fibers. The lower RaDeCC efficiency for cartridges may be caused by the texture. The cartridge texture may influence the emanation efficiency of  $^{220}\text{Rn}$  (Sun and Torgersen, 1998).

### 3.3 Influence of cartridge moisture contents on the RaDeCC efficiency

The RaDeCC detector efficiency is the product of the cell efficiency, system efficiency and emanation efficiency (Sun and Torgersen, 1998). Changes in the sample shape (fiber or cartridge) will not influence the cell efficiency and system efficiency. Sun and Torgersen (1998) suggested that the emanation efficiency was related to the thickness of water film on the  $\text{MnO}_2$ -coated fiber and that the RaDeCC efficiency for  $\text{MnO}_2$ -coated fibers was the highest at a water content of 0.3–1. We, thus, deduced that the RaDeCC efficiency for  $\text{MnO}_2$ -coated cartridges might be also affected by the moisture content of the cartridge. To determine a proper moisture content for the  $\text{MnO}_2$ -coated cartridge, the

moisture content of the cartridge standards was adjusted by sprinkling water or ventilating in a clean hood, and then left for a week to reach stability. First, we started with a moisture content of approximately 1 to avoid the water being carried into the scintillation cell. After measurements, the standards were placed in a clean hood to lower the moisture content by about 5%, then measuring and lowering moisture content until the moisture content of the cartridge standards reached 0. As shown in Fig. 5, when the moisture content ranged from 0.04 to 1.04, the RaDeCC detector efficiency of System 3 for Cartridge Standard 1 fluctuated slightly, from 0.322 to 0.355 (with an average of  $0.335 \pm 0.009$  and RSD of 0.026). However, when the moisture content was less than 0.01, the efficiency showed a sharp decline to as low as 0.215 (Fig. 5a). The RaDeCC detector efficiency of System 4 for Cartridge Standard 2 showed a similar pattern with the efficiency in the range from 0.303 to 0.322 (with an average of  $0.312 \pm 0.005$  and RSD of 0.016) at a moisture content of 0.01–1.05 (Fig. 5b). As a result, with a moisture content of 0.05–1, the influence of moisture contents on the RaDeCC detector efficiency for cartridge standards was negligible.

### 3.4 Improvement in the pretreatment of the $\text{MnO}_2$ -coated cartridge

After the measurement of  $^{224}\text{Ra}$ , the  $\text{MnO}_2$ -coated cartridges were measured for  $^{226}\text{Ra}$  and  $^{228}\text{Ra}$ . In the common method, the  $\text{MnO}_2$ -coated acrylic cartridge was usually ashed at  $820^\circ\text{C}$  for 48 h (Henderson et al., 2013; Charette et al., 2015; Kipp et al., 2018). Then the ash was transferred to polystyrene vials and sealed with epoxy resin before being measured using HPGe (Henderson et al., 2013). The details of long-lived radium measurement and calculation with HPGe can be found in Moore (1984). However, ashing overnights (48 h) was time-consuming. In addition, about

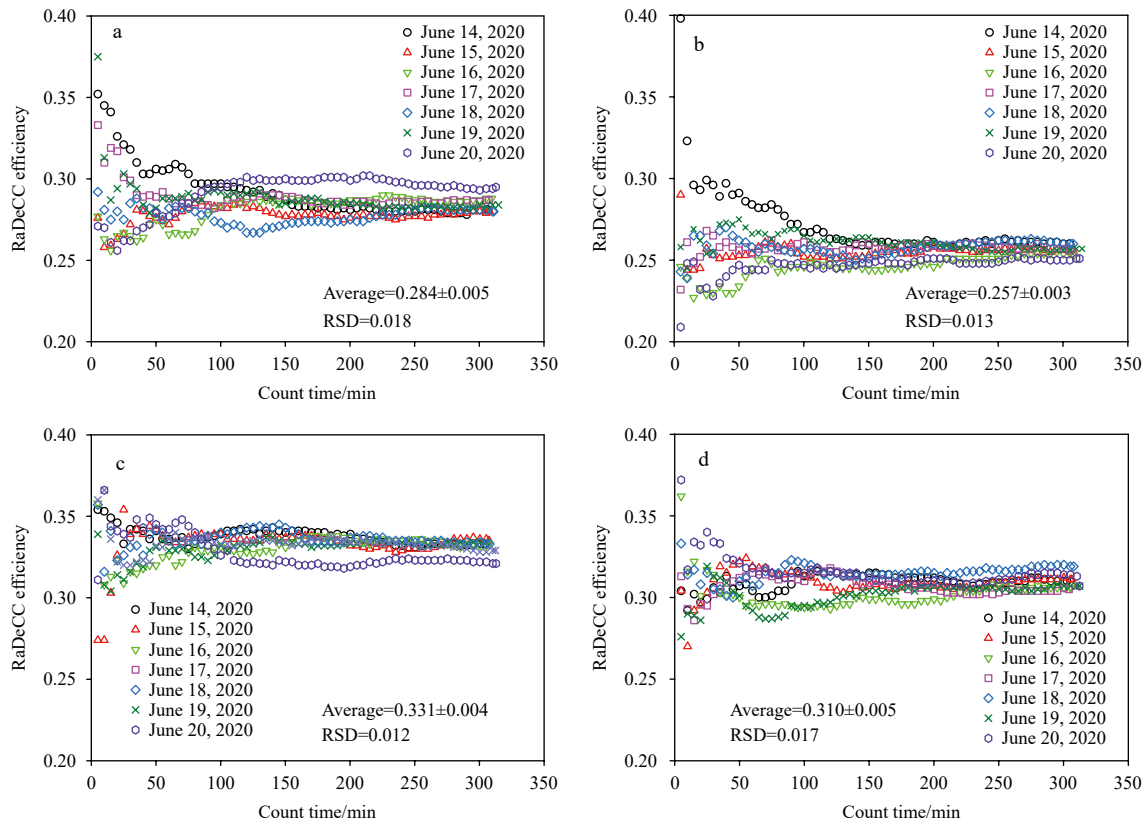
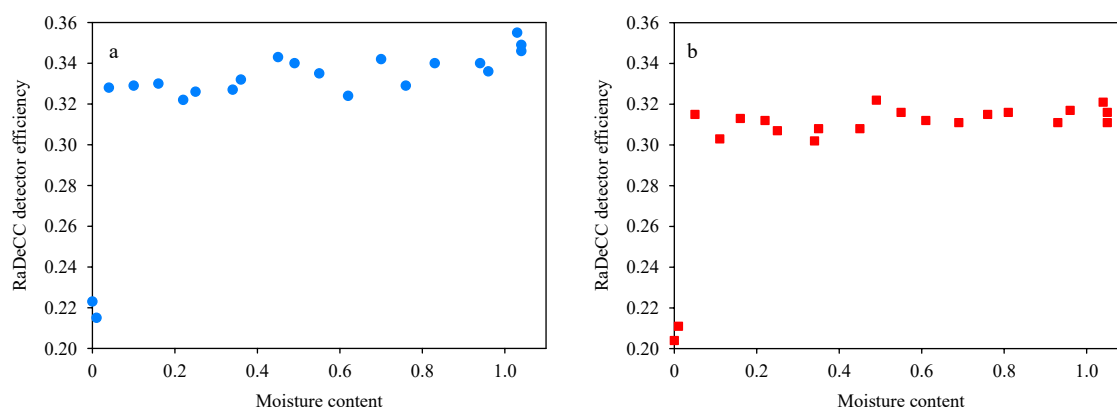


Fig. 4. RaDeCC efficiencies for four cartridge standards versus count time. a. System 1; b. System 2; c. System 3; d. System 4. Average denotes the average efficiency at 285 min. “ $\pm$ ” indicates one standard deviation. RSD represents the relative standard deviation.



**Fig. 5.** RaDeCC detector efficiencies versus moisture contents of the  $\text{MnO}_2$ -coated cartridge. a. Cartridge Standard 1 measured using System 3; b. Cartridge Standard 2 measured using System 4.

15% of ash is to be lost during transfer. And the weights of ash showed great variations, which can cause a change in the efficiency of HPGe of 25%. In our study, it took 6 h to completely ash the polypropylene cartridge, 42 h shorter than the acrylic cartridge. We did a comparative experiment using the acrylic cartridge and ashed for 6 h. The amount of ash of the acrylic cartridge was about a few times greater than that of our cartridge (Fig. S3). To avoid ash loss during transfer and the variation in the efficiency of HPGe caused by different ash weights, a pre-treatment method was developed. The ashed cartridge was leached and radium was coprecipitated with  $\text{BaSO}_4$  with details described in Section 2.3.

### 3.5 Determination of conversion factor for HPGe

Moore (1984) proposed a single factor ( $F$ ) to convert  $cpm$  to  $dpm$  as below:

$$dpm = F \times cpm, \quad (1)$$

where  $dpm$  is a unit of radioactive activity, disintegrations per minute. And  $cpm$  is the count rate of the instrument, counts per minute.  $F$  is related to the sample geometry in the measurement vial. In order to determine  $F$ ,  $^{226}\text{Ra}$  and  $^{228}\text{Ra}$  mixed standards were made. Weighed  $^{226}\text{Ra}$  and  $^{228}\text{Ra}$  standard solutions (National Institute of Metrology, China) were diluted to 600 mL and  $^{226}\text{Ra}$  and  $^{228}\text{Ra}$  were coprecipitated with  $\text{BaSO}_4$ , then the precipitate was filtered, sealed in centrifuge tubes, and measured using HPGe. Duplicate mixed standards were made and measured three times, respectively.  $F$  was consistent for the duplicate standards (Table S1).

### 3.6 Recovery of $^{226}\text{Ra}$ and $^{228}\text{Ra}$

During ashing, leaching, coprecipitation, and filtration (Fig. 2), potential loss of radium may occur. To determine the recovery of  $^{226}\text{Ra}$  and  $^{228}\text{Ra}$  during these processes, three  $\text{MnO}_2$ -coated cartridge standards were made in almost the same way as in the  $^{224}\text{Ra}$  standards preparation except that the long-lived radium isotopes in the residual liquid and washed RO water were coprecipitated with  $\text{BaSO}_4$ , then sealed in a matching vial. Three weeks later, the vial with  $\text{BaSO}_4$  precipitates was put in HPGe to measure for  $^{226}\text{Ra}$  and  $^{228}\text{Ra}$ . No peaks were detected for the vial, suggesting that all the  $^{226}\text{Ra}$  and  $^{228}\text{Ra}$  were absorbed on the  $\text{MnO}_2$ -coated cartridge. Three  $^{226}\text{Ra}$  and  $^{228}\text{Ra}$  cartridge standards were made and preprocessed as described in Section 2.3. The recovery ranged from 94% to 99% for  $^{226}\text{Ra}$  and from 100% to 102% for  $^{228}\text{Ra}$  (Table S2), greater than 85% in the study of Xie et

al. (1994). We also conducted an experiment to test the recovery of direct transferring the ash to the measurement vial. After ashing, the weight of the ashed cartridge in the cup was 3.4 g. After being transferred from the cup to the measurement vial, 0.5 g ash was lost. The recovery of the transfer was thus 85%. This indicates that our approach improved the recovery by 11%.

### 3.7 The influence of flow rates on the radium extraction efficiency of the $\text{MnO}_2$ -coated cartridge

Baskaran et al. (1993) revealed that the radium adsorption efficiency of the  $\text{MnO}_2$ -coated cartridge depended on the distribution coefficient of radium between the seawater and the  $\text{MnO}_2$ , the reaction rate between the radium and  $\text{MnO}_2$ , and the flow rate that controls the contact time. The radium extraction efficiency of the  $\text{MnO}_2$ -coated fiber was low at a flow rate greater than 1.5 L/min during sampling (Moore, 2008). As for  $\text{MnO}_2$ -coated cartridges, however, they are installed in *in situ* pumps with a flow rate of 4–7 L/min during sampling. To evaluate the influence of flow rates on the radium extraction efficiency of the  $\text{MnO}_2$ -coated cartridge, the nearshore seawater with different radium activities was pumped through a  $\text{MnO}_2$ -coated cartridge with a flow jet at different flow rates (Table S3), followed by 16 g  $\text{MnO}_2$ -coated fiber with a flow rate of less than 1 L/min (Fig. S4). Specific flow rates and the radium activities absorbed on cartridges and fibers were listed in Table S3. The  $^{224}\text{Ra}$  extraction efficiency decreased from 98% at 0.6 L/min to 73% at 7.8 L/min, then kept constant at around 77% (Fig. 6). Similar to the efficiency for  $^{224}\text{Ra}$ , the  $^{228}\text{Ra}$  extraction efficiency reduced from 100% to 79% with the flow rate changing from 0.6 L/min to 7.8 L/min, then

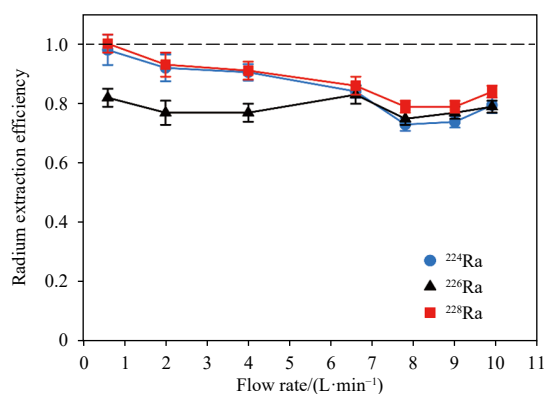


**Fig. 6.** The radium extraction efficiency of the  $\text{MnO}_2$ -coated cartridge versus the filtration rate.

kept constant at 82%. The extraction efficiency for  $^{226}\text{Ra}$  did not change much with flow rates, ranging from 75% to 83%. However, its peak was not observed at the lowest flow rate. Strangely, the extraction efficiency for  $^{226}\text{Ra}$  differed from those for  $^{224}\text{Ra}$  and  $^{228}\text{Ra}$  at 0.6–6.6 L/min for some reason that we have not figured out yet. To summarize, the *in situ* pump working flow rate, 4–7 L/min, contributed 3%–4% variation to the radium extraction efficiency of the  $\text{MnO}_2$ -coated cartridge. The error in the extraction efficiency caused by the measurement error of radium ranged from 2% to 6% (Table S3). The uncertainty in the radium extraction efficiency caused by the flow rate fell in the range of this error.

#### 4 Conclusions

In this study, we made improvements in enrichment and pretreatment of low-activity radium in the open ocean. Firstly, the commonly used acrylic cartridge was replaced by a cheaper polypropylene cartridge. Our cartridge took only 6 h to be ashed, much shorter than that for the acrylic cartridge. Secondly, a circulation system with a hot acidic  $\text{KMnO}_4$  solution was designed to coat the polypropylene cartridge with  $\text{MnO}_2$ . In this way, a homogeneous coating was realized with a radium extraction efficiency 20%–61% higher than that of the commonly used direct immersion in the same solution. Thirdly, after ashing the cartridge, we leached the ash with a mixture of hydroxylamine hydrochloride and HCl, then coprecipitated radium with  $\text{BaSO}_4$  in order to avoid potential ash loss during transfer and the change in the efficiency of HPGe caused by the variation in the ash weight. The recovery of these processes ranged from 94% to 102%, which improves over those in previous studies.

Moreover, the RaDeCC efficiency was not sensitive to the moisture content of our  $\text{MnO}_2$ -coated cartridge. Within the working flow rate of the *in situ* pump, about 4–7 L/min, the radium extraction efficiency of our  $\text{MnO}_2$ -coated cartridge only varied from 3%–4%, well within the uncertainty resulting from the measurement errors.

#### Acknowledgements

We would like to thank Shilei Jin and Wen Lin for sampling. We thank Hotel Hongzhuancuo for providing the field experiment site.

#### References

- Baskaran M, Murphy D J, Santschi P H, et al. 1993. A method for rapid *in situ* extraction and laboratory determination of Th, Pb, and Ra isotopes from large volumes of seawater. *Deep-Sea Research Part I: Oceanographic Research Papers*, 40(4): 849–865, doi: [10.1016/0967-0637\(93\)90075-E](https://doi.org/10.1016/0967-0637(93)90075-E)
- Charette M A, Morris P J, Henderson P B, et al. 2015. Radium isotope distributions during the US GEOTRACES North Atlantic cruises. *Marine Chemistry*, 177: 184–195, doi: [10.1016/j.marchem.2015.01.001](https://doi.org/10.1016/j.marchem.2015.01.001)
- Charette M A, Splivallo R, Herbold C, et al. 2003. Salt marsh submarine groundwater discharge as traced by radium isotopes. *Marine Chemistry*, 84(1–2): 113–121
- Henderson P B, Morris P J, Moore W S, et al. 2013. Methodological advances for measuring low-level radium isotopes in seawater. *Journal of Radioanalytical and Nuclear Chemistry*, 296(1): 357–362, doi: [10.1007/s10967-012-2047-9](https://doi.org/10.1007/s10967-012-2047-9)
- Kaufman A, Trier R M, Broecker W S, et al. 1973. Distribution of  $^{228}\text{Ra}$  in the world ocean. *Journal of Geophysical Research*, 78(36): 8827–8848, doi: [10.1029/JC078i036p08827](https://doi.org/10.1029/JC078i036p08827)
- Kipp L E, Sanial V, Henderson P B, et al. 2018. Radium isotopes as tracers of hydrothermal inputs and neutrally buoyant plume dynamics in the deep ocean. *Marine Chemistry*, 201: 51–65, doi: [10.1016/j.marchem.2017.06.011](https://doi.org/10.1016/j.marchem.2017.06.011)
- Ku T L, Li Y H, Mathieu G G, et al. 1970. Radium in the Indian-Antarctic Ocean south of Australia. *Journal of Geophysical Research*, 75(27): 5286–5292, doi: [10.1029/JC075i027p05286](https://doi.org/10.1029/JC075i027p05286)
- Michel J, Moore W S, King P T. 1981.  $\gamma$ -Ray spectrometry for determination of radium-228 and radium-226 in natural waters. *Analytical Chemistry*, 53(12): 1885–1889, doi: [10.1021/ac00235a038](https://doi.org/10.1021/ac00235a038)
- Moore W S. 1969. Measurement of  $\text{Ra}^{228}$  and  $\text{Th}^{228}$  in sea water. *Journal of Geophysical Research*, 74(2): 694–704, doi: [10.1029/JB074i002p00694](https://doi.org/10.1029/JB074i002p00694)
- Moore W S. 1972. Radium-228: Application to thermocline mixing studies. *Earth and Planetary Science Letters*, 16(3): 421–422, doi: [10.1016/0012-821X\(72\)90161-6](https://doi.org/10.1016/0012-821X(72)90161-6)
- Moore W S. 1976. Sampling  $^{228}\text{Ra}$  in the deep ocean. *Deep-Sea Research and Oceanographic Abstracts*, 23(7): 647–651, doi: [10.1016/0011-7471\(76\)90007-3](https://doi.org/10.1016/0011-7471(76)90007-3)
- Moore W S. 1984. Radium isotope measurements using germanium detectors. *Nuclear Instruments and Methods in Physics Research*, 223(2–3): 407–411
- Moore W S. 1996. Large groundwater inputs to coastal waters revealed by  $^{226}\text{Ra}$  enrichments. *Nature*, 380(6575): 612–614, doi: [10.1038/380612a0](https://doi.org/10.1038/380612a0)
- Moore W S. 2008. Fifteen years experience in measuring  $^{224}\text{Ra}$  and  $^{223}\text{Ra}$  by delayed-coincidence counting. *Marine Chemistry*, 109(3–4): 188–197
- Moore W S, Arnold R. 1996. Measurement of  $^{223}\text{Ra}$  and  $^{224}\text{Ra}$  in coastal waters using a delayed coincidence counter. *Journal of Geophysical Research: Oceans*, 101(C1): 1321–1329, doi: [10.1029/95JC03139](https://doi.org/10.1029/95JC03139)
- Moore W S, Reid D F. 1973. Extraction of radium from natural waters using manganese-impregnated acrylic fibers. *Journal of Geophysical Research*, 78(36): 8880–8886, doi: [10.1029/JC078i036p08880](https://doi.org/10.1029/JC078i036p08880)
- Rama, Todd J F, Butts J L, et al. 1987. A new method for the rapid measurement of  $^{224}\text{Ra}$  in natural waters. *Marine Chemistry*, 22(1): 43–54, doi: [10.1016/0304-4203\(87\)90047-8](https://doi.org/10.1016/0304-4203(87)90047-8)
- Sanial V, Kipp L E, Henderson P B, et al. 2018. Radium-228 as a tracer of dissolved trace element inputs from the Peruvian continental margin. *Marine Chemistry*, 201: 20–34, doi: [10.1016/j.marchem.2017.05.008](https://doi.org/10.1016/j.marchem.2017.05.008)
- Sun Yin, Torgersen T. 1998. The effects of water content and Mn-fiber surface conditions on  $^{224}\text{Ra}$  measurement by  $^{220}\text{Rn}$  emanation. *Marine Chemistry*, 62(3–4): 299–306
- Tan Ehui, Wang Guizhi, Moore W S, et al. 2018. Shelf-scale submarine groundwater discharge in the Northern South China Sea and East China Sea and its geochemical impacts. *Journal of Geophysical Research: Oceans*, 123(4): 2997–3013, doi: [10.1029/2017JC013405](https://doi.org/10.1029/2017JC013405)
- Trier R M, Broecker W S, Feely H W. 1972. Radium-228 profile at the second Geosecs intercalibration station, 1970, in the North Atlantic. *Earth and Planetary Science Letters*, 16(1): 141–145, doi: [10.1016/0012-821X\(72\)90249-X](https://doi.org/10.1016/0012-821X(72)90249-X)
- Wang Guizhi, Han Aiqin, Chen Liwen, et al. 2018. Fluxes of dissolved organic carbon and nutrients via submarine groundwater discharge into subtropical Sansha Bay, China. *Estuarine, Coastal and Shelf Science*, 207: 269–282
- Wang Guizhi, Jing Wenping, Wang Shuling, et al. 2014. Coastal acidification induced by tidal-driven submarine groundwater discharge in a coastal coral reef system. *Environmental Science & Technology*, 48(22): 13069–13075
- Wang Guizhi, Wang Zhangyong, Zhai Weidong, et al. 2015. Net submarine estuarine export fluxes of dissolved inorganic C, N, P, Si, and total alkalinity into the Jiulong River Estuary, China. *Geochimica et Cosmochimica Acta*, 149: 103–114, doi: [10.1016/j.gca.2014.11.001](https://doi.org/10.1016/j.gca.2014.11.001)
- Xie Yongzhen, Huang Yipu, Shi Wenyuan, et al. 1994. Simultaneous concentration and determination of  $^{226}\text{Ra}$ ,  $^{228}\text{Ra}$  in natural waters. *Journal of Xiamen University: Natural Science (in Chinese)*, 33(S1): 86–90
- Zhang Yan, Santos I R, Li Hailong, et al. 2020. Submarine groundwater discharge drives coastal water quality and nutrient budgets at small and large scales. *Geochimica et Cosmochimica Acta*, 290: 201–215, doi: [10.1016/j.gca.2020.08.026](https://doi.org/10.1016/j.gca.2020.08.026)

---

## Supplementary information:

**Fig. S1.** The acidic  $\text{KMnO}_4$  solution-circulating system to prepare  $\text{MnO}_2$ -coated cartridges. The circulating system was composed of a silicone tube, a holder, a submersible pump (JP-064, SUNSUN, China), a beaker, and a water bath (HH-8, Bangxi, China).

**Fig. S2.** RaDeCC efficiencies for  $^{224}\text{Ra}$  fiber standard versus count time. System 1 (a), System 2 (b), System 3 (c), and System 4 (d). Average denotes the average efficiency at 285 min. “ $\pm$ ” indicates one standard deviation. RSD represents the relative standard deviation.

**Fig. S3.** Acrylic cartridge ash (a) and polypropylene cartridge ash (b) after 6-h ashing.

**Fig. S4.** The process of testing the radium extraction efficiencies of  $\text{MnO}_2$ -coated cartridges.

**Table S1.** Conversion factors ( $F$ ) determined for HPGe. TS1 and TS2 are duplicate standards.

**Table S2.** The recovery of  $^{226}\text{Ra}$  and  $^{228}\text{Ra}$  during the pretreatment of  $\text{MnO}_2$ -coated cartridges.

**Table S3.** Flow rates and the activity of radium absorbed on  $\text{MnO}_2$ -coated cartridges and fibers, and the radium extraction efficiency of  $\text{MnO}_2$ -coated cartridges.

The supplementary information is available online at <https://doi.org/10.1007/s13131-023-2152-3> and <http://www.aosocean.com/>. The supplementary information is published as submitted, without typesetting or editing. The responsibility for scientific accuracy and content remains entirely with the authors.

SGD to respond to any treatment, so the outcome may take days, months, or even years to be seen.

On the nation-wide scale, we extrapolated our bay-wide SGD-carried nutrient fluxes to the entire Chinese coastline using the median SGD-carried nutrient fluxes (Table S6, SM) considering bays with small, medium, and large areas where SGD-associated nutrient fluxes are available. Notably, most investigations in Table S6 including ours were conducted in only one season. Considering that seasonal variations of SGD-associated nutrient fluxes may be present, additional uncertainties may be introduced in our extrapolation, which would be reduced by further investigations in more seasons. In the present extrapolation process, we assumed that there was no seasonal variation of SGD-carried nutrient fluxes. The total nutrient flux ( $\text{mol day}^{-1}$ ) via SGD along the Chinese coastline is  $(2.57 \pm 1.07) \times 10^8$  for DIN,  $(3.21 \pm 1.36) \times 10^6$  for SRP, and  $(1.49 \pm 0.26) \times 10^8$  for DSi. Our results are comparable to the total nutrient flux estimate of Zhang et al. (2020b). Despite the relatively small sizes of individual small bays, the great cumulative area as well as the greater area-normalized SGD-carried nutrient flux makes the total DIN contribution from SGD in small bays approximately twice as much as that in large bays (Figure 8B). Therefore, investigations in small bays are critical to accurately estimate the SGD-associated nutrient fluxes and to assess the biogeochemical and environmental impacts of SGD along the entire Chinese coast.

From a global perspective, small bays may similarly contribute a significant amount of nutrients to coastal waters because their greater area-normalized SGD-carried nutrient fluxes and limited riverine inputs and therefore may likely play a disproportionately big role in local and national coastal systems. Thus, SGD-carried nutrients in small bays merit attention in environmental monitoring and management. A better understanding of the biogeochemical impacts of SGD in small bays is indispensable in future environmental investigations. Such investigations will definitely contribute to the United Nations Decade of Ocean Science for Sustainable Development (2021-2030; <https://en.unesco.org/ocean-decade>) in terms of understanding land- and sea-based sources of pollutants and contaminants and their potential impacts on ocean ecosystems.

## 5 Conclusions

We carried out station-based and underway mappings, as well as a 12-h time-series investigation in subtropical Dongshan Bay, China, to investigate the role that SGD plays in small bays ( $<500 \text{ km}^2$ ). We found the most significant positive correlations ( $P < 0.01$ ,  $R^2 > 0.90$ ) in global coastal ecosystems ever investigated between concentrations of the SGD tracer,  $^{228}\text{Ra}$ , and nutrients in Dongshan Bay, which revealed that the nutrient concentration was predominantly controlled by SGD on a bay-wide scale. Furthermore, SGD seemed to support the productivity of phytoplankton in the bay, as shown by the significant positive correlation ( $P = 0.02$ ,  $R^2 > 0.40$ ) between concentrations of  $^{228}\text{Ra}$  and Chl. *a*. Additional evidence of the support of SGD was that the highest biomass observed during the underway survey occurred where the highest activity of  $^{228}\text{Ra}$  was found in the station-based mapping, implying the support of SGD-carried nutrients to algal blooms. On the bay-wide scale, the SGD-carried nutrient fluxes ( $\text{mmol day}^{-1}$ ) were  $(7.06 \pm 0.82) \times 10^5$ ,  $(2.05 \pm$

$0.34) \times 10^4$ , and  $(1.12 \pm 0.34) \times 10^6$  for DIN, SRP, and DSi, respectively, which accounted for over 95% of the nutrient sources. After extrapolating our results to the entire Chinese coast, the SGD-carried DIN flux in small bays was approximately twice as much as those in large bays ( $>2,000 \text{ km}^2$ ), highlighting the importance of small bays in estimating the role that SGD plays in coastal nutrient distribution and budgets on a national scale.

## Data availability statement

The original contributions presented in the study are included in the article/Supplementary Material. Further inquiries can be directed to the corresponding authors.

## Author contributions

All authors listed have made a substantial, direct, and intellectual contribution to the work and approved it for publication.

## Funding

This research was supported by the Natural Science Foundation of Fujian Province of China (grant no. 2019J01020) and the National Natural Science Foundation of China (grant no. 42188102, 41576074).

## Acknowledgments

We thank the crew of Mindongyu 63093 for their industrious work. We also thank the technicians at the Dongshan Swire Marine Station, Xiamen University for their technical support.

## Conflict of interest

The authors declare that the research was conducted in the absence of any commercial or financial relationships that could be construed as a potential conflict of interest.

## Publisher's note

All claims expressed in this article are solely those of the authors and do not necessarily represent those of their affiliated organizations, or those of the publisher, the editors and the reviewers. Any product that may be evaluated in this article, or claim that may be made by its manufacturer, is not guaranteed or endorsed by the publisher.

## Supplementary material

The Supplementary Material for this article can be found online at: <https://www.frontiersin.org/articles/10.3389/fmars.2023.1164589/full#supplementary-material>